Research article

Hao Hu, Dongliang Gao, Xiao Lin, Songyan Hou, Baile Zhang, Qi Jie Wang* and Yu Luo*

Directing Cherenkov photons with spatial nonlocality

https://doi.org/10.1515/nanoph-2020-0135
Received February 20, 2020; accepted April 21, 2020;
published online May 23, 2020

Abstract: Cherenkov radiation in natural transparent materials is generally forward-propagating, owing to the positive group index of radiation modes. While negative-index metamaterials enable reversed Cherenkov radiation, the forward photon emission from a swift charged particle is prohibited. In this work, we theoretically investigate emission behaviours of a swift charged particle in the nanometallic layered structure. Our results show that Cherenkov photons are significantly enhanced by longitudinal plasmon modes resulting from the spatial nonlocality in metamaterials. More importantly, longitudinal Cherenkov photons can be directed either forward or backward, stringently depending on the particle velocity. The enhanced flexibility to route Cherenkov photons holds promise for many practical applications of Cherenkov radiation, such as novel free-electron radiation sources and new types of Cherenkov detectors.

Keywords: Cherenkov radiation; light–matter interaction; metamaterials; plasmonics; spatial nonlocality.

***Corresponding authors: Qi Jie Wang and Yu Luo**, School of Electrical and Electronic Engineering, Nanyang Technological University, Nanyang Avenue, Singapore, 639798, Singapore, E-mail: qjwang@ntu.edu.sg (Q.J. Wang); luoyu@ntu.edu.sg (Y. Luo). https://orcid.org/0000-0002-9910-1455 (Q.J. Wang); https://orcid.org/0000-0003-2925-682X (Y. Luo)
Hao Hu: School of Electrical and Electronic Engineering, Nanyang Technological University, Nanyang Avenue, Singapore, 639798, Singapore. https://orcid.org/0000-0003-2892-1971
Dongliang Gao: School of Physical Science and Technology, Soochow University, Suzhou, 215006, China
Xiao Lin and Baile Zhang: Division of Physics and Applied Physics, School of Physical and Mathematical Sciences, Nanyang Technological University, Singapore, 637371, Singapore
Songyan Hou: University of Arizona, James C. Wyant College of Optical Sciences, Tucson, AZ, 85721, USA

1 Introduction

Cherenkov radiation refers to the physical effect that a charged particle with a velocity exceeding the phase velocity of light in a medium can emit coherent photons at a constant angle [1, 2]. According to the theory developed by I. Frank and I. Tamm in 1937, the radiation angle θ_c relative to the particle trajectory is intimately dependent on the particle velocity v as $\cos(\theta_c) = v_{th}/v$, where $v_{th} = v/n$ is the threshold velocity (i. e., the phase velocity of light in the medium with the refractive index n) [3].

A wide controllability of radiation angles is preferable for many practical applications of Cherenkov radiation, e. g., improving the flexibility to direct photon emissions from free-electron radiation sources or enhancing the sensitivity of Cherenkov detectors [4–12]. However, Cherenkov radiation in natural transparent materials is generally forward-propagating, because of the positive group velocity of radiation modes. To overcome this problem, researchers come up with numerous negative-index metamaterials to manipulate Cherenkov radiation [13–18]. The recent theoretical and experimental studies show that radiation directions can be reversed when a swift charged particle interacts with left-handed metamaterials, hyperbolic metamaterials, or plasmonic waveguides [19–21]. Even so, the radiation angle of Cherenkov photons is still limited in a relatively narrow angular band, i. e., negative angles relative to the particle velocity. A novel mechanism that can enable to direct Cherenkov photons in a broader range, e. g., from a positive angle to a negative angle, is highly desirable.

In this work, we theoretically demonstrate that the spatial nonlocality provides an opportunity to flexibly control emission behaviours of a swift charged particle in a nanometallic layered structure. In the nonlocal treatment, the quantum-sized metallic structure supports longitudinal plasmon modes above the bulk plasmon frequency of metals [22, 23]. These longitudinal modes originate from the nonlocal electron screening in metals. The swift charged particle in the nonlocal layered structure enables excitation of longitudinal modes at resonant frequencies, and emits longitudinal Cherenkov photons. Interestingly,

the sign of effective group index of longitudinal modes is dependent on the particle velocity in the nonlocal layered structure. With the consideration of realistic material loss, the effective group index is negative if the particle velocity is sufficiently large, while the effective group index is positive if the particle velocity is sufficiently small. Consequently, the variation of particle velocity enables us to route longitudinal Cherenkov photons in backward-propagating direction or forward-propagating direction at will.

2 Modelling Cherenkov radiation in the nanometallic layered structure

We begin with the theoretical model of Cherenkov radiation in the nanometallic layered structure. Without the loss of generality, we consider a charged particle with the velocity of $\bar{v}_0$ moves in the air. The particle trajectory is parallel to and close to the top surface of layered structure made of periodic metal slabs, as shown in Figure 1. The thickness of metal slab is d_1, the gap width between metal stabs is d_2, and thus the pitch of layered structure is $P = d_1 + d_2$. In this work, we define the radiation angle θ_r as the angle between the y-axis and corresponding Poynting power vector of radiation modes.

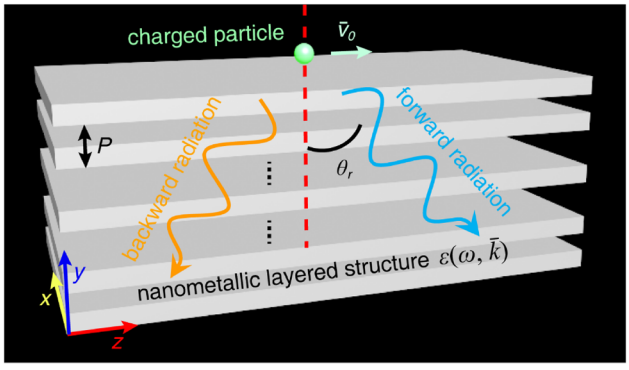

Figure 1: Schematic diagram of Cherenkov radiation in the nanometallic layered structure. A charged particle with the velocity of $\bar{v}_0$ moves on the top of nanometallic layered structure along the z-direction, generating longitudinal Cherenkov photons downward. The thicknesses of metal slabs and air slabs are d_1 and d_2, respectively. The pitch of layered structure is $P = d_1 + d_2$. The free-electron response of nonlocal metals is described with the hydrodynamic model as $\epsilon(\omega, \bar{k})$. Here, the radiation angle of longitudinal Cherenkov photons θ_r is defined as the angle between the Poynting power vector and the y-axis. Longitudinal Cherenkov photons are forward-propagating when $\theta_r > 0$ and backward-propagating when $\theta_r < 0$.

In the cylinder coordinate (ρ, φ, z), the current density of swift charged particle $\bar{J}^q(\bar{r}, t) = \hat{z} q_0 v \delta(\rho) \delta(z - vt)$, generates the charge field in the integral expressions as [24]

$$\bar{E}^q(\bar{r}, t) = \int_{-\infty}^{+\infty} \mathrm{d}\omega \frac{\mathrm{i} q_0 e^{\mathrm{i}k_z z} k_\rho}{8\pi\omega\epsilon_0} \left[k_z \mathrm{H}_1^{(1)}(k_\rho \rho)\hat{\rho} + \mathrm{i}k_\rho \mathrm{H}_0^{(1)}(k_\rho \rho)\hat{z} \right] e^{-\mathrm{i}\omega t}, \quad (1)$$

$$\bar{H}^q(\bar{r}, t) = \hat{\varphi} \int_{-\infty}^{+\infty} d\omega \frac{i q_0 k_\rho e^{ik_z z}}{8\pi} H_1^{(1)}(k_\rho \rho) e^{-i\omega t}. \quad (2)$$

Here ω is the angular frequency, $k_0 = \omega/c$, $k_z = \omega/v$, and $k_\rho = \sqrt{k_0^2 - k_z^2}$. To generalize our discussions, we introduce a scalar potential ϕ_0 (by noticing the transverse feature of fields emitted by a swift charged particle) and express the vacuum field in the frequency domain as,

$$\bar{E}^q(\bar{r}, \omega) = \frac{\mathrm{i}}{\omega\epsilon_0} \nabla \times \nabla \times (\hat{z}\phi_0), \quad (3)$$

$$\bar{H}^q(\bar{r}, \omega) = \nabla \times (\hat{z}\phi_0), \quad (4)$$

Comparing Eq. (1) and (2) with Eq. (3) and (4), we find that the potential of a swift charged particle along the z-axis takes the form of

$$\phi_0(\bar{r}, \omega) = \frac{\mathrm{i} q_0}{8\pi} \mathrm{H}_0^{(1)}(k_\rho \rho) \mathrm{e}^{\mathrm{i}k_z z} = \int_{-\infty}^{+\infty} \mathrm{d}k_x X_0 \mathrm{e}^{\mathrm{i}k_x x + \mathrm{i}k_{Ty1}|y| + \mathrm{i}k_z z}, \quad (5)$$

where the wavevector component $k_{Ty1} = (k_0^2 - k_x^2 - k_z^2)^{1/2}$ and the amplitude of the swift particle source $X_0 = \mathrm{i}q_0/(8\pi^2 k_{Ty1})$.

To illustrate the impact of nonlocal electron screening in metals on emission behaviours of the swift charged particle, we compare Cherenkov radiations in the local layered structure and nonlocal layered structure. The local description of light-matter interactions assumes that the induced surface charges only precisely reside on the boundary of metals. And as a result, the free-electron response of metals is transversal, given by Drude model as $\epsilon_T(\omega) = 1 - \omega_p^2/[\omega(\omega + i\gamma)]$, where ω_p is the bulk plasmon frequency, γ is the collision frequency. In the local treatment, we calculate the fields in all regions using potentials with decompositions of transverse magnetic field and transverse electric field. In the region j, the potentials of transverse magnetic field and transverse electric field take the form as

$$\phi_{TMj} = \int_{-\infty}^{+\infty} \mathrm{d}k_x \left(T_{TMj}^{+} e^{\mathrm{i}k_{Tyj}(y - y_j)} + R_{TMj}^{-} e^{-\mathrm{i}k_{Tyj}(y - y_{j+1})} \right) \mathrm{e}^{\mathrm{i}k_x x + \mathrm{i}k_z z}, \quad (6)$$

$$\phi_{TEj} = \frac{1}{\omega\varepsilon_0}\int_{-\infty}^{+\infty} \mathrm{d}k_x\Big(T_{TEj}^{+}\mathrm{e}^{\mathrm{i}k_{Tyj}(y-y_j)} + R_{TEj}{}^{-}\mathrm{e}^{-\mathrm{i}k_{Tyj}(y-y_{j+1})}\Big)\mathrm{e}^{\mathrm{i}k_x x+\mathrm{i}k_z z} \tag{7}$$

where $k_{Tyj} = (\epsilon_{rj}k_0^2 - k_x^2 - k_z^2)^{1/2}$ for metal slabs with $\epsilon_{rj} = \epsilon_T$ and air slabs with $\epsilon_{rj} = 1$. T_{TMj}^{+}, T_{TEj}^{+}, $R_{TMj}{}^{-}$, $R_{TEj}{}^{-}$ are scattering coefficients of transverse fields in the region j. The transverse radiation fields $\bar{E}_T^R$ and $\bar{H}_T^R$ are expressed in terms of the following two sets of scalar eigen functions [25]:

$$\overline{E}_T^R(\bar{r},\omega) = \frac{\mathrm{i}\bar{\varepsilon}_r^{-1}}{\omega\epsilon_0}\nabla\times\nabla\times(\hat{z}\phi_{TM}) - \nabla\times(\hat{z}\phi_{TE}), \tag{8}$$

$$\overline{H}_T^R(\bar{r},\omega) = \nabla\times(\hat{z}\phi_{TM}) + \frac{\mathrm{i}}{\omega\mu_0}\nabla\times\nabla\times(\hat{z}\phi_{TE}), \tag{9}$$

Under the local description, the boundary conditions are [26]

$$\hat{n}\times\Big[\overline{H}_{j-1}\big(y_j\big) - \overline{H}_j\big(y_j\big)\Big] = 0, \tag{10}$$

$$\hat{n}\times\Big[\overline{E}_{j-1}\big(y_j\big) - \overline{E}_j\big(y_j\big)\Big] = 0, \tag{11}$$

The method of transfer matrix is employed for the calculation of scattering coefficients [27].

However, a more accurate description of light-matter interactions takes the nonlocal electron screening in metals into account [28]. Owing to the quantum repulsion of electrons, the surface charge densities have a finite penetration inside metals. Such a spatial dispersion gives rise to a longitudinal response of metals, which can be theoretically described by the hydrodynamic model as $\epsilon_L(\bar{k}_L,\omega) = 1 - \omega_p^2/(\omega^2 + i\gamma\omega - \beta^2\bar{k}_L^2)$ [29], while the transverse response remains unchanged; Here, β is proportional to the Fermi velocity as $\beta = (3/5)^{1/2}$ and $\bar{k}_L$ is the wavevector of the longitudinal electric field as $|k_L| = [\omega(\omega+i\gamma) - \omega_p]^{1/2}/\beta$. To study the interplay between a swift charged particle and the nonlocal layered structure, we introduce an additional scalar potential for the longitudinal electric field in the metal of region j as

$$\phi_{Lj} = \frac{1}{\omega\varepsilon_0}\int_{-\infty}^{+\infty}\mathrm{d}k_x\Big(T_{Lj}^{+}\mathrm{e}^{\mathrm{i}k_{Lyj}(y-y_j)} + R_{Lj}{}^{-}\mathrm{e}^{-\mathrm{i}k_{Lyj}(y-y_{j+1})}\Big)e^{\mathrm{i}k_x x+\mathrm{i}k_z z}, \tag{12}$$

where $k_{Lyj} = (k_L^2 - k_x^2 - k_z^2)^{1/2}$. T_{Lj}^{+} and $R_{Lj}{}^{-}$ are scattering coefficients of longitudinal electric field in the region j. Thus, the longitudinal electric field can be obtained as

$$\overline{E}_L^R = \nabla\phi_{Lj}. \tag{13}$$

Especially, due to the existence of longitudinal electric field, an additional boundary condition, i. e., the longitudinal continuity of electric field, is applied at the boundary of metals $y = y_j$ as [30]

$$n\cdot\Big[\overline{E}_{j-1}\big(y_j\big) - \overline{E}_j\big(y_j\big)\Big] = 0 \tag{14}$$

We employ the method of transfer matrix to calculate all the scattering coefficients in each region of this configuration [31, 32]. Finally, Cherenkov radiation in the nonlocal layered structure is the superposition of transverse electric field, transverse magnetic field and longitudinal electric field.

In addition, to qualify the photon emission enhanced by longitudinal plasmon modes, we compute the energy loss density and photon extraction efficiency of a swift charged particle. The energy loss density is determined by employing power dissipation formula as [21]

$$G = \frac{q_0 v_0}{\pi\omega\varepsilon_0}\mathrm{Im}\left[\int_0^{+\infty}\mathrm{d}k_x\big(k_x^2 + k_{Ty1}^2\big)R_{TM1}^{+}\right], \tag{15}$$

where R_{TM1}^{+} is the reflection coefficient of transverse magnetic field. The photon extraction efficiency per second of the swift charged particle is obtained as [33]

$$\eta = \frac{dN/d\omega}{E_k}, \tag{16}$$

where $dN/d\omega = G/(\hbar\omega)$ is the radiation intensity per second and E_k is the kinetic energy of the charged particle.

3 Photon emission enhanced by longitudinal plasmon modes

In this section, we demonstrate that the photon emission from a swift charged particle is significantly enhanced by longitudinal plasmon modes in the quantum-sized layered structure. As a concrete example, we select the silver (Ag) as the metal, where ω_p = 9.0 eV, γ = 0.032 eV and $v_F = 136\times10^6$ m/s. The thickness of metal slab is d_1 = 2 nm, and the pitch of the layered structure is P = 6 nm. The number of the period in calculation is n = 10. In this configuration, the spatial nonlocality is strong as $d_1 \gtrsim \lambda_{TF}$, where $\lambda_{TF} \sim 5$ Å is the Tomas–Fermi screening length. When the particle velocity v_0/c = 0.5 and the studied wavelength is λ_0 = 129 nm, the photon emission is prohibited inside the local layered structure but appears only when $\lambda_0 > \lambda_p$, where the bulk plasmon wavelength $\lambda_p = (2\pi c)/\omega_p$ = 138 nm (Figure 2A) [34]. This is because, under the local description, the metal is no longer a plasmonic material as $\epsilon_T > 0$ when $\lambda_0 < \lambda_p$ as shown in the energy loss density spectrum in Figure 2C. The situation becomes quite different when the nonlocal electron

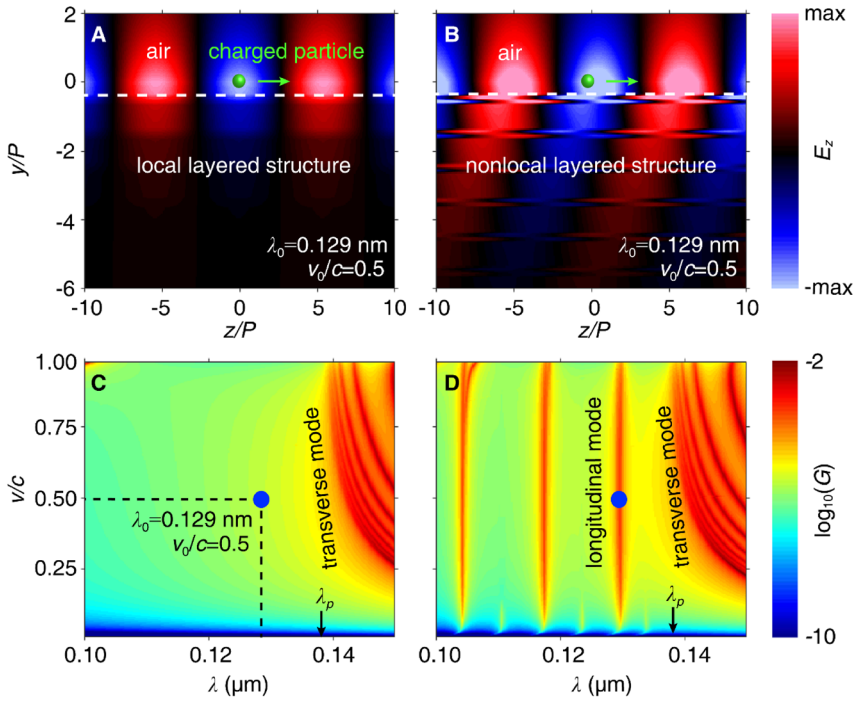

Figure 2: Photon emission enhanced by longitudinal plasmon modes. (A) and (B) The radiation patterns generated by a swift charged particle in the nanometallic layered structure, where the particle velocity is v_0 = 0.5 c and the studied wavelength is λ_0 = 0.129 μm. (C) and (D) The energy loss density spectra (G) of a swift charged particle in the layered structure versus the particle velocity v/c and the studied wavelength λ. In (A) and (C), the free-electron response of metals is in local approximation, while in (B) and (D), the free-electron response of metals in under the nonlocal description. λ_p = 138 nm is the bulk plasmon wavelength of metals in the study. The unit of energy loss density G is mW/eV.

screening in metals is considered. Because nonlocal metals can support longitudinal plasmon modes if $\lambda_0 < \lambda_p$, the coupling between the longitudinal plasmon modes results in the formation of bulk Bloch modes in the nonlocal layered structure at discrete resonant wavelengths, i. e., 129 nm, 117 nm, 104 nm, etc. (Figure 2D). Due to the enhanced photonic density of states, the swift charged particle can efficiently emit longitudinal Cherenkov photons at a resonant wavelength (Figure 2B). In addition, when the geometric size is comparable with the Tomas–Fermi screening length λ_{TF}, the longitudinal modes arising from the spatial nonlocality enable the enhancement of photon emission more than four orders of magnitude, compared with the local approximation (Figure 2D). However, when the geometric size is far beyond λ_{TF}, i. e., $d_1 \gg \lambda_{TF}$, the enhancement of photon emission is relatively weak [29].

4 Radiation angles of longitudinal Cherenkov photons

To reveal radiation angles of longitudinal Cherenkov photons, we investigate the isofrequency contours of bulk Block modes in the nonlocal layered structure [35]. The isofrequency contours in the lossless case show that the bulk Block modes appear only in a finite range of wavevectors (Figure 3A). When the wavevector is sufficiently small, the isofrequency contour is hyperboloid-shaped,

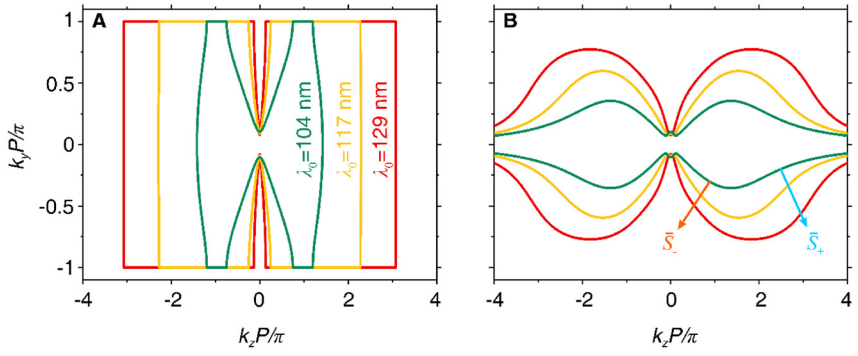

Figure 3: Isofrequency contours of bulk Block modes in the nanometallic layered structure. (A) The isofrequency contours when the realistic material loss is artificially neglected, i. e., γ = 0 eV. (B) The isofrequency contours when the realistic materials loss is considered, i. e., γ = 0.032 eV. The Poynting power vector is denoted as $\bar{S}_\pm$, where the subscripts represent the forward radiation and backward radiation, respectively. The studied wavelengths are 129, 117, and 104 nm respectively for (A) and (B), when longitudinal Cherenkov photons can be emitted by a swift charged particle.

indicating that the nonlocal layered structure enables negative refraction. When the wavevector is relatively large, the isofrequency becomes flat. As a consequence, the energy flow of bulk Block modes is normal relative to the interface. When the wavevector is sufficiently large, the isofrequency contour closes due to the decoupling of longitudinal plasmon modes in metal slabs. Beyond the wavevector cutoff, the bulk Block modes disappear. However, isofrequency contours of bulk Block modes are smoothen by taking the realistic material loss into account (Figure 3B). In the limit of small wavevectors, the isofrequency contour remains hyperbolic, while it becomes elliptical when the wavevector is sufficiently large. The exotic isofrequency contours indicate that the effective group index can be controlled in a flexible way. Taking the bulk Block mode at 129 nm for example, we find that the sign of effective group index is stringently dependent on the z-component wavevectors k_z. When $(k_z P)/\pi > 2$, the effective group index is positive. As a result, longitudinal Cherenkov photons are forward-propagating with $\bar{S} = \bar{S}_+$. However, when $(k_z P)/\pi < 2$, the effective group index becomes negative, leading to reversed longitudinal Cherenkov photons with $\bar{S} = \bar{S}_-$.

Properly engineering isofrequency contours enables us to sensitively control the radiation angles of longitudinal Cherenkov photons in a broad range of particle velocities, while the photon emission remains relatively intensive. The radiation angle here is calculated using $\theta_r = \mathrm{atan}(\mathrm{d}k_Z/\mathrm{d}k_y)$. Figure 4 shows the radiation angle spectra and extraction efficiency spectra at three resonant wavelengths of longitudinal modes as same in Figure 3. As shown in Figure 4A, the threshold velocity for longitudinal Cherenkov photons is $v_{\mathrm{th}} \approx 0.03c$. The appearance of the velocity threshold results from the spatial dispersion in nanometallic layered structures: For one thing, the finite structural size results in a wavevector cutoff, beyond which coupling between longitudinal plasmon modes in each metal slab is prohibited. For another, the nonlocal electron screening in metals gives rise to an effective thickness of metal slabs, whose value is slightly larger than the realistic thickness. Thus, the increased geometric size further reduces the wavevector cutoff. Even so, the threshold velocity for longitudinal modes is rather small, because of the deep-subwavelength unit cell of the periodic structure. In the end, the photon emission in the nonlocal layered structure can be enhanced in a broad range of particle velocities (Figure 4). The corresponding photon extraction efficiency is higher for longitudinal Cherenkov photons at a larger resonant wavelength. Moreover, the spatial nonlocality allows the radiation angle of longitudinal Cherenkov photons to be controlled from a positive value to a negative value with the variation of particle velocity (Figure 4). In particular, at the resonant wavelength $\lambda_0 = 129$ nm, there is a relatively wide controllability of radiation angles (Figure 3A). When the particle velocity $v_0 = 0.03c$, the corresponding radiation angle is $\theta_r = 28.7°$. With the increase of the particle velocity, the photon emission is gradually changed to the backward-propagating direction. When the particle velocity approaches to the light velocity in the vacuum $(v_0 \to c)$, the radiation angle of longitudinal Cherenkov photons reaches a low-bound value of −52.2°. In particular, when the particle velocity is $v_0 = 0.05c$, the swift charged particle emits longitudinal Cherenkov photons in a direction perpendicular to the interface of nanometallic layered structure. The underlying reason is that balanced by the spatial dispersion and realistic material loss, the excited longitudinal plasmon modes have a zero group velocity along the interface. Therefore, the energy of longitudinal Cherenkov photons is downward-propagating only.

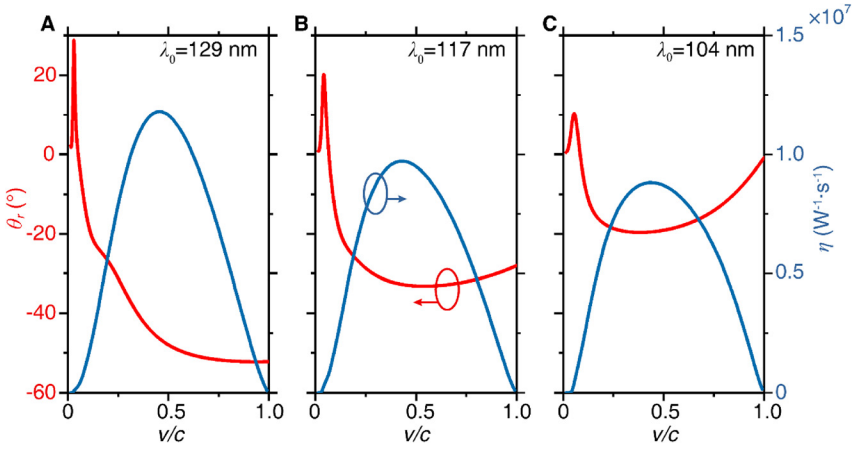

Figure 4: Emission behaviours of a swift charged particle in the nanometallic layered structure. (A)–(C) The radiation angle spectra θ_r (red line) and the photon extraction efficiency per second η (blue line) as the function of particle velocity v/c. The studied wavelengths λ_0 of longitudinal Cherenkov photons are 129 nm in (A), 117 nm in (B), and 104 nm in (C) respectively when longitudinal Cherenkov photons can be emitted by a swift charged particle.

5 Applications

The feasibility to direct Cherenkov photons in a broad range of angles facilitates many practical applications of Cherenkov radiation. On the one hand, an electron beam traveling in the nanometallic layered structure can be employed for an integrated free-electron radiation source by coupling longitudinal Cherenkov photons from the nanometallic layered structure to the far field. The novel free-electron radiation source is capable of generating forward-propagating photons and backward-propagating photons, switched by the particle velocity. On the other hand, since the photon emission is enhanced in a broad range of particle velocities, to which the radiation angle of longitudinal Cherenkov photons is sensitive, our configuration extends the momentum range for the sensitive determination of particle velocity or particle identification. For example, the calculated radiation angle θ_r of longitudinal Cherenkov photons is dependent on the momenta p and the rest masses of charged particles (Figure 5). When p = 0.04 GeV/c, electron, proton, pion, and kaon would emit longitudinal Cherenkov photons in angles of −52.2°, −33.6°, −11.8°, and 5.1°, respectively. The giant differences among radiation angles indicate that the broad controllability of longitudinal Cherenkov photons enhances the sensitivity to determine particle velocities and discriminate charged particles in an extended momentum range.

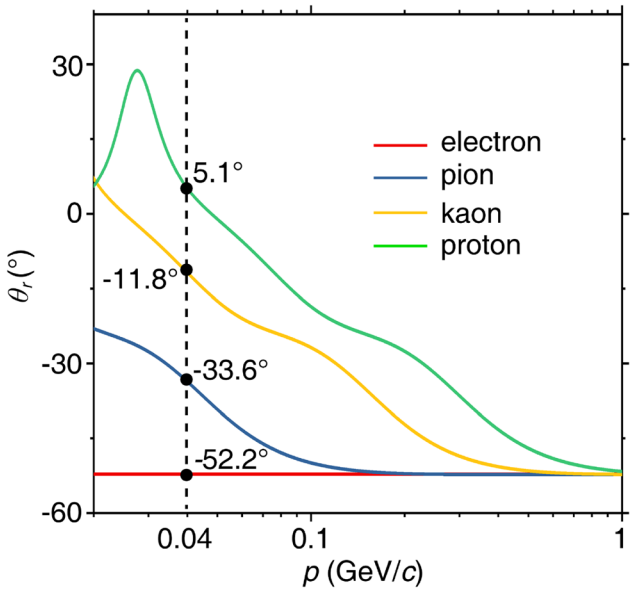

Figure 5: Radiation angles θ_r of longitudinal Cherenkov photons versus particle momenta p.For comparison, four types of swift charged particles are studied, i. e., electron, pion, kaon, and proton. When the momentum of charged particles is p = 0.04 GeV/c, the radiation angles θ_r of longitudinal Cherenkov photons emitted by the electron, pion, kaon, and proton are −52.2°, −33.6°, −11.8°, and 5.1° respectively. The studied wavelength is 129 nm, when longitudinal Cherenkov photons can be emitted by swift charged particles.

6 Conclusion

To conclude, we theoretically demonstrate that the spatial nonlocality in metamaterials provides a new degree of freedom to direct Cherenkov photons. Particularly, longitudinal plasmon modes resulting from the spatial nonlocality in nanometallic layered structure enhance the photon emission for four orders in a broad range of particle velocities above the bulk plasmon wavelength of metals, where Cherenkov photons are generally believed to be prohibited in the local approximation. In contrast to emission behaviours of a swift charged particle in natural transparent materials and negative-index metamaterials, the nonlocal layered structure could direct longitudinal Cherenkov photons in both the forward-propagating direction and backward-propagating direction. Meanwhile, our calculation results show that the radiation angle of longitudinal Cherenkov photons is sensitively controlled by the particle velocity. In addition, owing to the available large mode refractive index for longitudinal modes, the threshold velocity for longitudinal Cherenkov photons is relatively small, facilitating the particle identification or determination of particle velocity in an extended momentum range. This work enriches the theory of Cherenkov radiation and offers a new insight to control emission behaviours of a swift charged particle [36–41].

Acknowledgments: Y. Luo was partly sponsored by Singapore Ministry of Education under Grant No. MOE2018-T2-2-189 (S), MOE2017-T1-001-239 (RG91/17 (S)); A*STAR AME programmatic Grant No. A18A7b0058; Q. J. Wang was partly sponsored by funding from the Ministry of Education, Singapore (Grant Nos. MOE2016-T2-2-159 and MOE2018-T2-1-176), the National Research Foundation Singapore, Competitive Research Program (No. NRF-CRP18-2017-02). D. Gao was partly sponsored by National Natural Science Foundation of China (Grant No. 11504252).
Competing interests: The authors declare no competing financial interests.
Data and materials availability: All data needed to evaluate the conclusions in the paper are present in the paper.

References

[1] P.A. Čerenkov, "Visible radiation produced by electrons moving in a medium with velocities exceeding that of light," *Phys. Rev.*, vol. 52, p. 378, 1937, https://doi.org/10.1103/PhysRev.52.378.

[2] P. A. Čerenkov, "Visible light from pure liquids under the impact of γ-rays," *Dokl. Acad. Sci. URSS*, vol. 2, pp. 451–457, 1934, https://doi.org/10.3367/UFNr.0093.196710n.0385.

[3] I. E. Tamm and I. M. Frank, "Coherent radiation of fast electrons in a medium," *Dokl. Acad. Sci. URSS*, vol. 14, pp. 107–112, 1937, https://doi.org/10.3367/UFNr.0093.196710o.0388.

[4] T. Ypsilantis and J. Séguinot, "Theory of ring imaging Cherenkov counters," *Nucl. Instrum. Meth. A*, vol. 343, pp. 30–51, 1994, https://doi.org/10.1016/0168-9002(94)90532-0.

[5] J. J. Aubert, U. Becker, P. J. Biggs, et al., "Experimental observation of a heavy particle," *J. Phys. Rev. Let.*, vol. 33, p. 1404, 1974, https://doi.org/10.1103/PhysRevLett.33.1404.

[6] C. Roques-Carmes, S. E. Kooi, Y. Yang, et al., "Towards integrated tunable all-silicon free-electron light sources," *Nat. commun.*, vol. 10, pp. 1–8, 2019, https://doi.org/10.1038/s41467-019-11070-7.

[7] The LHCb Collaboration, "The LHCb detector at the LHC," *J. Instrum.*, vol. 3, p. S08005, 2008, https://doi.org/10.1088/1748-0221/3/08/S08005.

[8] Z. Su, B. Xiong, Y. Xu, et al., "Manipulating Cherenkov radiation and smith–purcell radiation by artificial structures," *Adv. Opt. Mater.*, vol. 7, p. 1801666, 2019, https://doi.org/10.1002/adom.201801666.

[9] S. Liu, P. Zhang, W. Liu, et al., "Surface polariton Cherenkov light radiation source," *Phys. Rev. Lett.*, vol. 109, p. 153902, 2012, https://doi.org/10.1103/PhysRevLett.109.153902.

[10] C. Roques-Carmes, N. Rivera, J. D. Joannopoulos, M. Soljačić, and I. Kaminer, "Nonperturbative quantum electrodynamics in the Cherenkov effect," *Phys. Rev. X*, vol. 8, 2018, Art no. 041013, https://doi.org/10.1103/PhysRevX.8.041013.

[11] Z. Wang, K. Yao, M. Chen, H. Chen, and Y. Liu, "Manipulating Smith–Purcell emission with babinet metasurfaces," *Phys. Rev. Lett.*, vol. 117, p. 157401, 2016, https://doi.org/10.1103/PhysRevLett.117.157401.

[12] L. Jing, Z. Wang, X. Lin, et al., "Spiral field generation in Smith-Purcell radiation by helical metagratings," *Research*, vol. 2019, p. 3806132, 2019, https://doi.org/10.34133/2019/3806132.

[13] Z. Duan, X. Tang, Z. Wang, et al., "Observation of the reversed Cherenkov radiation," *Nat. Commun.*, vol. 8, pp. 1-7, 2017, https://doi.org/10.1038/ncomms14901.

[14] C. Luo, M. Ibanescu, S. G. Johnson, and J. D. Joannopoulos, "Cerenkov radiation in photonic crystals," *Science*, vol. 299, pp. 368–371, 2003, https://doi.org/10.1126/science.1079549.

[15] J. Lu, T. M. Grzegorczyk, Y. Zhang, et al., "Čerenkov radiation in materials with negative permittivity and permeability," *Opt. Express.*, vol. 11, pp. 723–34, 2003, https://doi.org/10.1364/oe.11.000723.

[16] W. Liu, "Generalized magnetic mirrors," *Phys Rev Lett*, vol. 119, p. 123902, 2017, https://doi.org/10.1103/PhysRevLett.119.123902.

[17] P. V. Kapitanova, P. Ginzburg, F. J. Rodríguez-Fortuño, et al., "Photonic spin Hall effect in hyperbolic metamaterials for polarization-controlled routing of subwavelength modes," *Nat. Commun.*, vol. 5, pp. 1–8, 2014, https://doi.org/10.1038/ncomms4226.

[18] J. Li, L. Fok, X. Yin, G. Bartal, and X. Zhang, "Experimental demonstration of an acoustic magnifying hyperlens," *Nat. Mater.*, vol. 8, pp. 931–934, 2009, https://doi.org/10.1038/nmat2561.

[19] Xi S., Chen H., Jiang T., Ran L., et al., "Experimental verification of reversed Cherenkov radiation in left-handed metamaterial," *Phys. Rev. Lett.*, vol. 103, p. 194801, 2009, https://doi.org/10.1103/PhysRevLett.103.194801.

[20] F. Liu, L. Xiao, Y. Ye, Wang M., et al., "Integrated Cherenkov radiation emitter eliminating the electron velocity threshold," *Nat. Photon.*, vol. 11, pp. 289–292, 2017, https://doi.org/10.1038/nphoton.2017.45.

[21] J. Tao, Q. J. Wang, J. Zhang, and Y. Luo, "Reverse surface-polariton Cherenkov radiation," *Sci. Rep.*, vol. 6, p. 30704, 2016, https://doi.org/10.1038/srep30704.

[22] H. Hu, J. Zhang, S. A. Maier, and Y. Luo, "Enhancing third-harmonic generation with spatial nonlocality," *ACS Photon.*, vol. 5, pp. 592–598, 2017, https://doi.org/10.1021/acsphotonics.7b01167.

[23] R. J. Pollard, A. Murphy, W. R. Hendren, et al., "Optical nonlocalities and additional waves in epsilon-near-zero metamaterials," *Phys. Rev. Lett.*, vol. 102, p. 127405, 2009, https://doi.org/10.1103/PhysRevLett.102.127405.

[24] J. A. Kong, *Theory of Electromagnetic Waves*, New York, Wiley-Interscience, 1975.

[25] B. Zhang, H. Chen, B. I. Wu, Y. Luo, L. Ran, and J. A. Kong, "Response of a cylindrical invisibility cloak to electromagnetic waves," *Phys. Rev. B*, vol. 76, p. 121101, 2007, https://doi.org/10.1103/PhysRevB.76.121101.

[26] H. Hu, L. Liu, X. Hu, D. Liu, and D. Gao, "Routing emission with a multi-channel nonreciprocal waveguide," *Photon. Res.*, vol. 7, pp. 642–646, 2019, https://doi.org/10.1364/PRJ.7.000642.

[27] F. Krayzel, R. Pollès, A. Moreau, M. Mihailovic, and G. Granet, "Simulation and analysis of exotic non-specular phenomena," *J. Eur. Opt. Soc.-Rapid*, vol. 5, p. 10025, 2010, https://doi.org/10.2971/jeos.2010.10025.

[28] Y. Yang, D. Zhu, W. Yan, et al., "A general theoretical and experimental framework for nanoscale electromagnetism," *Nature*, vol. 576, p. 248–252, 2019, https://doi.org/10.1364/FIO.2019.FTu6A.1.

[29] C. Ciracì, R. T. Hill, J. J. Mock, et al., "Probing the ultimate limits of plasmonic enhancement," *Science*, vol. 337, p. 1072–1074, 2012, https://doi.org/10.1126/science.1224823.

[30] S. Raza, G. Toscano, A. P. Jauho, M. Wubs, and N. A. Mortensen, "Unusual resonances in nanoplasmonic structures due to nonlocal response," *Phys. Rev. B*, vol. 84, p. 121412, 2011, https://doi.org/10.1103/PhysRevB.84.121412.

[31] J. Benedicto, R. Pollès, C. Ciracì, E. Centeno, D. R. Smith, and A. Moreau, "Numerical tool to take nonlocal effects into account in metallo-dielectric multilayers," *J. Opt. Soc. Am. A*, vol. 32, pp. 1581–1588, 2015, https://doi.org/10.1364/JOSAA.32.001581.

[32] A. Moreau, C. Ciraci, and D. R. Smith, "Impact of nonlocal response on metallodielectric multilayers and optical patch antennas," *Phys Rev B*, vol. 87, 2013, Art no. 045401, https://doi.org/10.1103/PhysRevB.87.045401.

[33] A. Massuda, C. Roques-Carmes, Y. Yang, et al., "Smith–Purcell radiation from low-energy electrons," *ACS Photon.*, vol. 5, pp. 3513–3518, 2018, https://doi.org/10.1021/acsphotonics.8b00743.

[34] A. V. Zayats, I. I. Smolyaninov, and A. A. Maradudin, "Nano-optics of surface plasmon polaritons," *Phys. Rep.*, vol. 408, pp. 131–314, 2005, https://doi.org/10.1016/j.physrep.2004.11.001.

[35] W. Yan, M. Wubs, and N. A. Mortensen, "Hyperbolic metamaterials: nonlocal response regularizes broadband supersingularity," *Phys. Rev. B*, vol. 86, p. 205429, 2012, https://doi.org/10.1103/PhysRevB.86.205429.

[36] V. Ginis, J. Danckaert, I. Veretennicoff, and P. Tassin, "Controlling Cherenkov radiation with transformation-optical metamaterials," *Phys. Rev. Lett.*, vol. 113, p. 167402, 2014, https://doi.org/10.1103/PhysRevLett.113.167402.

[37] P. Genevet, D. Wintz, A. Ambrosio, A. She, R. Blanchard, and F. Capasso, "Controlled steering of Cherenkov surface plasmon wakes with a one-dimensional metamaterial," *Nat. Nanotechnol.*, vol. 10, pp. 804–809, 2015, https://doi.org/10.1038/nnano.2015.137.

[38] X. Lin, S. Easo, Y. Shen, et al., "Controlling Cherenkov angles with resonance transition radiation," *Nat. Phys.*, vol. 14, pp. 816–821, 2018, https://doi.org/10.1038/s41567-018-0138-4.

[39] N. V. Sapra, K. Y. Yang, D. Vercruysse, et al., "On-chip integrated laser-driven particle accelerator," *Science*, vol. 367, pp. 79–83, 2020, https://doi.org/10.1126/science.aay5734.

[40] Y. Yang, A. Massuda, C. Roques-Carmes, et al., "Maximal spontaneous photon emission and energy loss from free electrons," *Nat. Phys.*, vol. 14, pp. 894–899, 2018, https://doi.org/10.1038/s41567-018-0180-2.

[41] K. Koshelev, G. Favraud, A. Bogdanov, Y. S. Kivshar, and A. Fratalocchi, "Nonradiating photonics with resonant dielectric nanostructures," *Nanophotonics*, vol. 8, pp. 725–745, 2019, https://doi.org/10.1515/nanoph-2019-0024.